Contents lists available at ScienceDirect

Optical Materials

journal homepage: http://www.elsevier.com/locate/optmat





Determining the refractive index and the dielectric constant of PPDT2FBT thin film using spectroscopic ellipsometry

Chandan Howlader a, Mehedhi Hasan Alex Zakhidov b, Maggie Yihong Chen chandan Howlader A, Mehedhi Hasan Alex Zakhidov b, Maggie Yihong Chen b, Chandan Howlader B, Mehedhi Hasan B, Alex Zakhidov b, Maggie Yihong Chen b, Chandan Howlader B, Mehedhi Hasan B, Alex Zakhidov b, Maggie Yihong Chen b, Chandan Howlader B, Mehedhi Hasan B, Alex Zakhidov b, Maggie Yihong Chen b, Chandan Howlader B, Mehedhi Hasan B, Alex Zakhidov b, Maggie Yihong Chen b, Chen B,

- ^a Materials Science Engineering, and Commercialization, Texas State University, San Marcos, TX, 78666, USA
- ^b Department of Physics, Texas State University, San Marcos, TX, 78666, USA
- ^c Ingram School of Engineering, Texas State University, San Marcos, TX, 78666, USA

ARTICLE INFO

Keywords:
PPDT2FBT
Optical dispersion
Spectroscopic ellipsometry
Refractive index
Extinction coefficient

ABSTRACT

Despite the recent increase in PPDT2FBT polymer thin film applications for optoelectronic devices, a comprehensive study of this material's optical dispersion properties is unavailable. The optical properties of the PPDT2FBT thin film is investigated using variable-angle spectroscopic ellipsometry (VASE) at ambient conditions. Knowledge of optical dispersion properties is essential for designing and fabricating optoelectronic devices such as solar cells, photodetectors, and photodiodes. In this research, we determined the dielectric function of PPDT2FBT thin film using the B-spline model and then reproduced the dielectric function using Psemi-Tri oscillators. We estimated the refractive index (n) of the thin film to be between 2.00 and 2.15 and the extinction coefficient (k) to be in the range of 1.14–1.39 at a wavelength of 632.8 nm. We further verified the estimated optical properties from the model using directly measured quantities such as transmission and absorption data obtained using the ultraviolet–visible (UV–Vis) spectrometer and thicknesses obtained using a surface profilometer. In addition, we determined the optical band gap of PPDT2FBT using the absorption coefficient.

1. Introduction

poly[(2,5-bis(2-hexyldecyloxy)phenylene)-alt-(5,6-Recently. difluoro-4,7-di(thiophen-2-yl) benzo[c] thiadiazole)] [1,2,5](PPDT2FBT) polymer material has attracted the attention of the scientific community [1]. The PPDT2FBT polymer has a balanced electron hole mobility and semi-crystalline properties [2]. In addition, the device made of PPDT2FBT polymer remains thermally stable for 200 h at 130 °C. Most importantly, the polymer does not lose solution processability because of its strong interchain interaction. It has also been shown to have a photocurrent extraction efficiency close to unity and a higher fill factor, even for thick film [1]. These attributes make this material a good candidate for applications in optoelectronic devices such as solar cells [1,3,4], photo-diodes [5], organic field-effect transistors [6], and photo-detectors [3,7,8]. PPDT2FBT is also a suitable material for low-cost solution-processable fabrication technologies [9].

In designing optoelectronic devices, optical properties such as the refractive index, band gap, dielectric coefficient, absorption coefficient, and extinction coefficient play significant roles [10,11]. The value of refractive index of a material facilitates the numerical analysis of a device based on that material [12]. Specially, for light emitting diodes

(LEDs), it is an important property to do the proper modeling for angular dependence of emission and light extraction [13]. Furthermore, the refractive index has a significant role to determine the external and internal efficiency of polymeric organic LEDs [10] and the anti-reflection efficiency of a material [14]. Ellipsometry is widely used as nondestructive measurement technique to measure the film properties from light material interaction. Hence, other film attributes such as thickness, roughness, bandgap, electronic transition behavior etc. can be derived. Therefore, study the optical properties of thin film using ellipsometry enables the numerical design of efficient optoelectronic device [15]. While the optical properties of popular polymers such as P3HT, PTB7 and their composition were studied [16], to the best of our knowledge, the optical properties of PPDT2FBT have not been studied comprehensively. Our group did preliminary work on PPDT2FBT to study the optical properties [17]. We believe a thorough study of those properties is critical for newer applications such as, anti-reflection coatings and interfacial layers [18]. For multilayer optical devices, the optical constants of individual layers are critical to controlling the light passing through the device as well as the charge carrier transport [19,20]. Historically, spectroscopic ellipsometry (SE) has been the technique of choice for determination of optical constants nondestructively [21]. SE

E-mail address: chandanqumar@gmail.com (C. Howlader).

^{*} Corresponding author.

has been used for decades for this purpose [18]. SE technique measures the ratio (ρ) of the perpendicular (r_s) and parallel (r_p) components of the light reflected from the interfaces, as shown in Equation (1) below [21]:

$$\rho = \frac{r_p}{r_s} = \tan(\psi) exp(i\Delta) \tag{1}$$

where ψ (Psi) is the amplitude ratio and Δ (Delta) is the phase difference of r_p and $r_s.$

However, optical modeling is particularly challenging for spincoated films due to interfacial roughness. The anomalous nature of dispersion in such films creates additional complexity in modeling efforts [22]. Additionally, the multiple fitting probabilities of SE data for different conditions is another challenge to estimate the refractive index and extinction coefficient accurately. For instance, a different substrate and a different process technique could change the optical properties [23]. In this research, we studied the optical properties of PPDT2FBT thin film.

2. Experimental methods

2.1. Sample preparation

PPDT2FBT thin films were deposited on a glass substrate using spin coating. The schematic diagram of this film is shown in Fig. 1(a) and Fig. 1(b) shows the chemical structure of the PPDT2FBT polymer [2]. The PPDT2FBT was dissolved in O-xylene, stirred at 400 rpm on a hotplate at 70 $^{\circ}\text{C}$ overnight, and then kept at in-situ conditions for 24 h. We made films with different thicknesses by changing the spin speed and the material concentration. A detailed description of the sample preparation process presented in the sample preparation section of supplementary documentation.

2.2. Sample characterization

The thin films were characterized for the wavelength range of 300 nm–900 nm using VASE (J.A. Woollam Co. M2000) and an UV–Vis spectrometer (UV 2600 from SHIMADZU) was used to retrieve the optical properties. A profilometer (KLA Tencor P7) and atomic force microscope (Bruker Dimension ICON) was used to determine the average thickness and roughness, respectively. To remove the backside reflection from the back of the glass substrate, we pasted black tape on the backside which is a common practice for reflective substrate.

2.3. SE modeling

The Psi (Ψ) and Delta (Δ) obtained from the SE measurement were required to be fitted with a suitable model to identify the optical and physical properties. We used the CompleteEASE software that comes with the J.A. Woollam Co. Spectroscopic Ellipsometer Package to perform the modeling. First, the SE data that consisted of the Ψ and Δ spectra of the glass substrate were fitted using a Cauchy equation for the wavelength range of 300 nm–900 nm with a known thickness of $\sim\!\!1$ mm.

Acceptability of the model is identified by the goodness of fit. The goodness of fit is represented by a term named Means-Squared Error (MSE) and it is defined in equation (2) [15].

$$MSE_{NCS} = \sqrt{\frac{1}{3n - m} \sum_{i=1}^{n} \left[\left(\frac{N_{Ei} - N_{Gi}}{0.001} \right)^{2} + \left(\frac{C_{Ei} - C_{Gi}}{0.001} \right)^{2} + \left(\frac{S_{Ei} - S_{Gi}}{0.001} \right)^{2} \right]}$$
(2)

where n is the number of wavelengths, m is the number of fit parameters, and $N = Cos(2\Psi)$, $C = Sin(2\Psi)Cos(\Delta)$, and $S = Sin(2\Psi)Sin(\Delta)$.

MSE defines the goodness of fit of the optical model with the measured data. For the fixed substrate thickness, a roughness of 1.79 \pm 0.02 nm was obtained for the glass slide with the MSE value of 2.19. Optical properties of glass substrate were used as the substrates' optical properties while modeling the PPDT2FBT/glass samples. The PPDT2FBT film shows highly absorptive behavior in the visible range as per UV–Vis absorption data.

To fit partially absorptive materials, B-spline is a suitable model in CompleteEASE Package for initial fitting of the SE data. This B-spline model consists of a basis set for polynomial splines and the "B" stands for basis. This model can determine the dielectric function of a material without any assumption of the functional form of light interaction with the thin film. Also, the B-spline parameterized dielectric functions give us the building block of parametrization with the oscillators. A simple recursion formula is used to model the B-splines and a set of Kramers-Kronig (KK) consistent basis functions can be obtained from this Bsplines [24]. The real dielectric ($\varepsilon_1(\omega)$) spectra of a material can be analytically calculated using the KK causality relationships once the imaginary dielectric ($\varepsilon_2(\omega)$) spectra of the material is parameterized by a B-spline curve. For each sample, we used the thickness measured with the profilometer and Root Mean Square (RMS) roughness as fixed parameters as we performed the global fitting of n and k for the ranges of 1-4 and 0 to 2, respectively. For simplicity, we did not turn on the KK fitting parameters at the beginning. The energy resolution of the B-spline model set to 0.05 eV. The B-spline model generated $\varepsilon_2(\omega)$ spectra for the energy range of 1 eV to 4 eV is added in the supplementary document. However, this model resulted in higher MSE. This prompted us to revisit the SE model to minimize the MSE value and, at the same time, determine if the n and k are physically meaningful. To deal with the substrate roughness, we introduced an effective medium approximation (EMA) layer between the PPDT2FBT thin film and the substrate [25]. Bruggeman EMA of 50% host material and 50% void can be used to well define the interfacial layer and that helps to properly model the SE data. Glass slide roughness was measured in the range of 1 nm to 2 nm. Initially, a fixed EMA layer thickness of 1 nm was with 50% composition was selected and allowed to fit the model. Furthermore, the EMA layer thickness was allowed to fit for a range of 1 nm to 2 nm at the next step of fitting the SE model. The use of the EMA layer reduced the MSE, particularly for the spectral range of 300 nm-900 nm. As developed model was applied for measuring the film thickness ranged from ~100 nm to \sim 305 nm. For this modeling procedure, the films were considered as isotropic and tried to fit within a minimum number of parameters at a

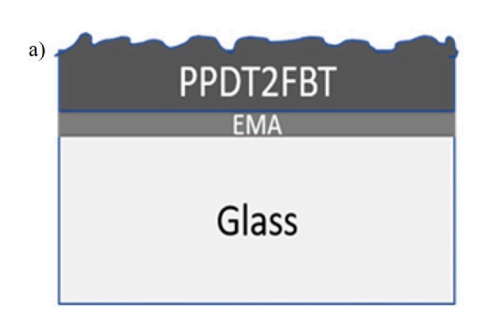


Fig. 1. a) Schematic diagram of PPDT2FBT thin film on glass substrate; b) chemical structure of PPDT2FBT polymer.

time. Yet, all the polymer thin films exhibit some degree of anisotropy depending on the thickness and the deposition process [23]. Therefore, PPDT2FBT polymer thin film might have some degree of anisotropy. However, Optical anisotropy of the PPDT2FBT sample is ignored in the model for simplicity and in future more detailed analyses of the anisotropic optical properties of this material are required.

The B-spline model provides us with the mathematically accurate description of the dielectric function, that we used as a steppingstone for the parameterization of PPDT2FBT by a general oscillator (GEN-OSC) method. We employed a summation of Psemi-Tri oscillators to parameterize the B-spline model generated real (ϵ_1) and imaginary (ϵ_2) dielectric functions for the PPDT2FBT film. The combination of Psemi-Tri oscillators can produce a highly flexible functional shape that is KK consistent. It is also a subset of the more general Herzinger-Johs Parameterized Semiconductor Oscillator function. Details explanation of the mathematical function of Psemi-Tri oscillator is given in somewhere else [26].

3. Results and discussions

The optical and physical properties of PPDT2FBT thin film have been measured for samples with thicknesses ranging from ~ 100 nm to ~ 300 nm for wavelengths ranging from 300 nm to 900 nm. As Fig. 1(a) shows, an EMA layer lies between the PPDT2FBT and the substrate, which is associated with the glass substrate's roughness. The thin film itself also has a surface roughness of \sim 1.3 nm shown in Fig. 2. The films for all samples measured in this study were deposited by following identical process on the same type of glass substrates. Understanding the interaction between thin films and light is essential for optical dispersion studies. In pursuit of that understanding, we performed UV-Vis spectroscopy on thin-film samples of different thicknesses. The absorbance of the PPDT2FBT thin films were obtained from UV-Vis spectrometer for the wavelength range of 300 nm to 900 nm. The spectrometer basically measures transmission spectra from the sample utilizing unpolarized light. We know that the absorbance is the inverse of transmittance, thus the spectrometer provides us the inverse result of the transmission spectra. For this analysis we mainly interested in absorption peaks. That is why, reflectance spectra were ignored. Fig. 3(a) shows the normalized absorption spectra of several samples. The absorption spectra were divided by its maximum value to get the normalized absorption spectra. The PPDT2FBT thin films exhibited mostly absorptive nature over the wavelength range of ~300 nm to ~700 nm with several local peaks and valleys. A sharp rise in absorption for all thicknesses was observed at \sim 700 nm. We also calculated the absorption coefficient (α) of a thin film of known thickness using the equation $\alpha = 2.303$ A/t, where (A) is absorbance and (t) is the thin-film thickness. From the absorption coefficient, we drew the Tauc plot of $(\alpha.h\nu)^{1/2}$ versus $(h\nu)$ and a tangent

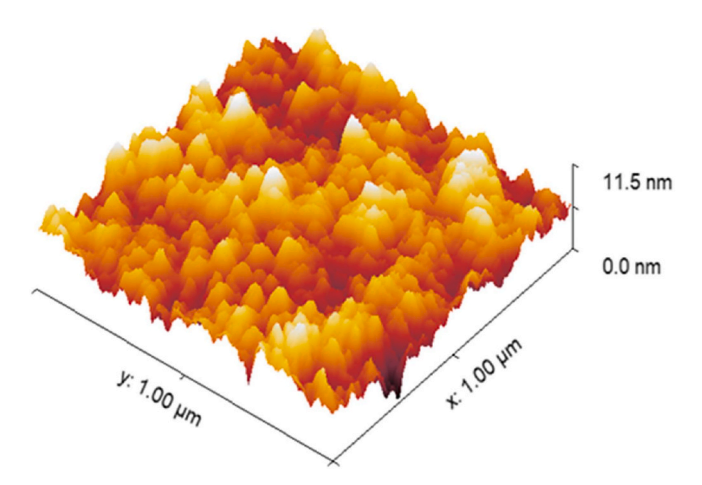


Fig. 2. AFM image of PPDT2FBT polymer thin film.

was drawn at the linear porting of the Tauc plot. Intersecting point of the tangent and energy represents the indirect allowed bandgap energy of ~ 1.70 eV, which is very close to the previously reported data [3]. The absorption peak positions were ~ 1.91 eV, ~ 2.08 eV, ~ 2.97 eV, and ~ 3.82 eV for different absorption intensity levels, and these peak positions were similar regardless of the film thickness. Most polymer materials show a wide absorption band for the visible and near-infrared region because of the localized π - π * and internal charge transition, that generate the peaks [3]. The absorption spectra also reveal information about electronic energy levels [27].

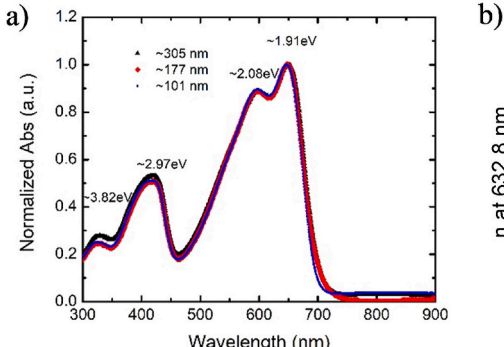
For accurate SE modeling of a thin film that has not been previously modeled, it requires some initial information to start with the modeling. The data extracted from the absorption coefficient or the absorption spectra are very useful for identifying a suitable SE model because such modeling depends highly on the sample's nature.

For SE modeling, the CompleteEASE analysis software offers several model packages for different types of thin film. For instance, B-spline is a popular model for partially or fully absorptive materials and it allows arbitrary flexibility in setting the refractive index and the extinction coefficient over the entire spectra. We chose B-spline for this preliminary model because the UV–Vis spectra describe the absorptive nature of PPDT2FBT film. The optical constants we estimated were calculated using this model's optimization parameters.

Like the optical constant estimation, a formulation of the dielectric function is crucial. Unlike most standard thin film, PPDT2FBT has an irregular dispersion profile (see Fig. S1, Fig. S2 and Fig. S3 in the supplementary documentation). Commonly used oscillator functions such as the Tauc-Lorentz or Cody-Lorentz functions are insufficient for rebuilding the complex dielectric function of this PPDT2FBT, which has multiple overlapping energy absorption centers. In contrast, the Psemi-Tri oscillator function offers some additional tuning parameters that are useful in building the complex dielectric function. For that reason, we rebuilt the optical constant obtained from the B-spline model as a sum of general Psemi-Tri oscillators (see research data). We verified the developed oscillator model by comparing the measured thickness to the thickness obtained from model. We used the MSE value to compare the goodness of fit for the models. Equation (2) shows the mathematical expression for the MSE [15,28]. The Psemi-Tri model estimated a \sim 296.70 nm thickness with an MSE of \sim 12 for a thin film with \sim 305.8 nm thickness (measured using the profilometer). The variations of the MSE and thickness compared to the B-spline model were ~ 2 and $\sim 1.3\%$, respectively. Even though the MSE value is relatively higher in the Psemi-Tri model, the measured thicknesses are within an acceptable range. The higher MSE value is not unusual for this kind of sample, that is, one with complex optical properties [21].

From Equation (2), we can conclude that the MSE value and the number of fit parameters have an inverse relationship. In our case, we used a minimum number of fit parameters, and this may be the reason for having a higher MSE value. We applied the same Psemi-Tri based GEN-OSC model to evaluate films with a wide range of thicknesses. It is worth mentioning that the literature contains evidence of thicknessdependent optical properties [29,30]. This suggests the possibility of thickness-dependent optical dispersion in the PPDT2FBT film. Thus, fitting the different thickness samples with a universal model produces a higher MSE value. With this in mind, we performed the B-spline global fitting for different film thicknesses. The individual fittings resulted in very similar optical constant profiles that exhibited gradual changes. Therefore, we modeled the SE data individually for each sample using the Psemi-Tri oscillator function. Table 1 above presents the thickness and MSE value obtained from GEN-OSC model by fitting the experimental data and the thicknesses obtained from the surface profilometer. Interestingly, we observed a gradual increase in the deviation in measured thickness for the smaller thicknesses, shown in Table 1. We also show the gradual refractive index change for wavelength 632.8 nm in Fig. 3(b) gained from the individual GEN-OSC fitting.

The thicknesses obtained from the GEN-OSC model stayed within



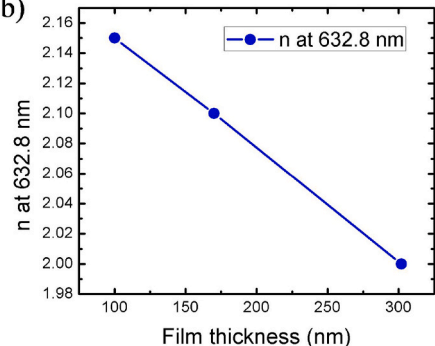


Fig. 3. a) Normalized absorption (Abs) spectra of PPDT2FBT from UV-Vis spectrometer; b) refractive index at 632.8 nm vs. thickness plot.

Table 1
MSE and thickness obtained from the GEN-OSC model and the thickness measured by profilometer of PPDT2FBT thin film are presented in this table.

Sample no.	MSE	SE Thickness (nm)	Profilometer Thickness (nm)	% Deviation
1	11.988	296.7 ± 1.4	305.8 ± 5.2	2.98
2	12.529	171.5 ± 0.6	177.8 ± 2.4	3.53
3	11.365	95.8 ± 0.6	101.6 ± 3.2	5.70

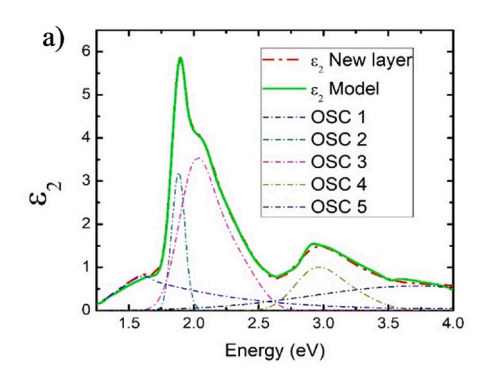
 \sim 6% of the thicknesses obtained with the surface profilometer. It can be seen clearly from Table 1 that the lower model thicknesses deviated more from the measured values. On the other hand, the MSE values demonstrate the model's goodness of fit to the experimental data. Generally, the accepted value of MSE is close to one [31]. However, for our samples, the MSE values were between \sim 11 and \sim 12. The acceptable thickness deviations obtained and the MSE values indicate the model's reliability as well as provide the extracted optical properties.

Fig. 4(a) shows the fitted GEN-OSC model for \sim 305 nm PPDT2FBT thin film with five Psemi-Tri oscillators. The number of oscillators depends on the number of peaks present in the absorption spectra and the peak positions of the modeled oscillators should be at the same positions as absorption peaks, which we can observe in Fig. 4(a). We used five oscillators to fit the optical constant. Table 2 presents the fitting parameters for the Psemi-Tri oscillator whereby the B-spline modeled dielectric function (ϵ_2) was fitted by the GEN-OSC model. The Psemi-Tri oscillator function has twelve parameters in total, seven of them are adjustable and five of them are fixed in terms of their value. In Table 2, A, E and B represent the amplitude, center energy and the broadening of the oscillator, respectively. Left and right-side width of the oscillator are represented by WL and WR with respect to the center energy. Other two parameters are relative magnitude of left and right control point and they are denoted by AL and AR, respectively. We justified this oscillator

model by matching the center energy position with the absorption spectra peaks shown in Fig. 3(a). Also, we obtained the band gap energy of $\sim\!1.70$ eV from the lowest energy transition of the Psemi-Tri oscillator model presented in Table 2 and it is similar to the determined bandgap energy from the absorption spectra. The inter-band transition defines the energy center, and the peak strength defines amplitude. We used several oscillator parameters to construct dielectric function. Note that there is a very minor energy peak in the near-infrared region at position $\sim\!1.4$ eV. We could also parameterize the layer with four oscillators if we ignored the absorption at energies below the bandgap energy.

We verified the extinction coefficient obtained from the GEN-OSC model by comparing it to the calculated extinction coefficient as it is known that the k has a relationship with the absorption coefficient. We calculated the extinction coefficient using the equation $k = \alpha \lambda / 4\pi$, where λ is the wavelength. We calculated the absorption coefficient (α) from the absorption spectra of the UV-Vis data. We plotted the calculated and modeled extinction coefficients for a wavelength range of 300 nm to 900 nm, as shown in Fig. 4(b). These coefficients agree with each other as the peak positions and the absorption edges are at the same positions. Hence, the accuracy of optical properties of PPDT2FBT thin film determined by SE model was verified. We note here, however, that the absorption properties may change depending on the sample-making conditions such as the materials concentration, the curing process, and the spin-coating recipe. Also, the reflectivity and interference effect change with changes in thickness, which results in variations in the extinction coefficient [27].

Besides extracting and verifying the k from the GEN-OSC model, we determined the n as shown in Fig. 5(a). The modeled n and k presented the most common characteristics of n and k. When there is no absorption, the k values should be zero and the n values should decrease with an increase of wavelength at the absorption edge. This relationship of n and k is a further verification of validity of the developed SE model [15]. Not all the samples provide the same values of n and k at a given



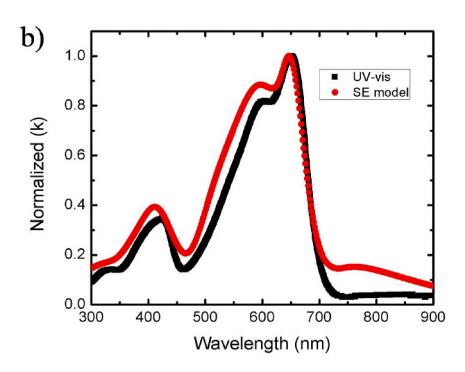


Fig. 4. a) GEN-OSC model derived from the SE model using Psemi-Tri oscillators; (b) extinction coefficient of PPDT2FBT derived from the SE model and calculated from the UV-Vis absorption.

Table 2 Dielectric function fitting parameters of P-Semi Tri oscillators obtained from B-spline model for \sim 305 nm PPDT2FBT thin film.

OSC no.	Α	B (eV)	E (eV)	WL (eV)	WR (eV)	AL	AR
OSC 1	$0.695\pm$	$0.011\pm$	$1.700\pm$	$0.500\pm$	5.97±	$0.752\pm$	0.050±
	0.004	0.004	0.007	0.004	0.11	0.004	0.004
OSC 2	4.98±	$0.0393 \pm$	$1.906\pm$	$0.122 \pm$	$0.0999 \pm$	$0.514\pm$	$0.114\pm$
	0.01	0.0003	0.001	0.002	0.0008	0.004	0.006
OSC 3	$3.752 \pm$	$0.121 \pm$	$2.05\pm$	$0.227 \pm$	$0.552 \pm$	$1.002 \pm$	$0.3894\pm$
	0.008	0.002	0.02	0.001	0.006	0.006	0.0004
OSC 4	$1.85 \pm$	$0.151 \pm$	$2.917 \pm$	$0.182 \pm$	$0.608\pm$	$0.43\pm$	$0.2751 \pm$
	0.02	0.006	0.002	0.003	0.007	0.02	0.0005
OSC 5	$1.460\pm$	$0.907\pm$	$3.66\pm$	$0.442 \pm$	$0.369 \pm$	$0.851 \pm$	$1.356\pm$
	0.002	0.007	0.03	0.005	0.002	0.008	0.004

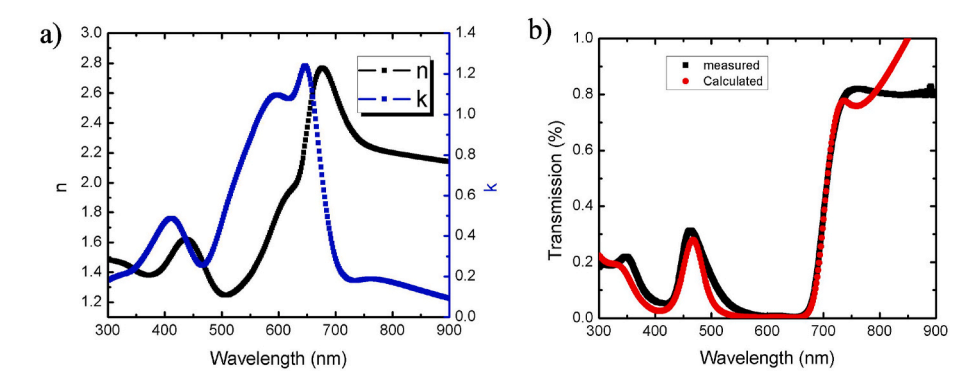


Fig. 5. a) Refractive index and extinction coefficient of PPDT2FBT obtained from the SE model; b) transmission spectra of PPDT2FBT thin film.

wavelength (see Fig. S7 in the supplementary document) because the refractive index and the extinction coefficient are affected by the film microstructure and the interchain interactions [10]. The obtained refractive indices and extinction coefficients vary between 2.00 and 2.15 and between 1.14 and 1.39, respectively, at the 632.8 nm wavelength when the thicknesses vary from $\sim\!305$ nm to $\sim\!100$ nm. The refractive index of the other commonly used polymer materials such as P3HT, PTB7 are respectively $\sim\!2.15$ and $\sim\!2.10$ [16,32]. Also, the n was tuned by making composition of P3HT and PTB7 with PCBM. The typical refractive index range of these polymers and compositions are between 2 and 2.15. The refractive index value obtained for PPDT2FBT lays very close to the range of the above-mentioned polymers.

To further test the reliability of the determined optical constants, we plotted the calculated transmission spectra using the n and k values obtained from the GEN-OSC model for the ~ 305 nm PPDT2FBT thin film and the n of the glass substrate for the wavelength range of 300 nm to 900 nm. We found that the measured transmission peaks and the calculated transmission peaks match closely for the most part of the spectra, as shown in Fig. 5(b).

Mismatches are observed for the calculated and measured transmission spectra at the UV and near-infrared regions. This mismatch of spectra can be attributed to the calculation error and the n and k taken from the GEN-OSC oscillator model. Fig. 5(a) also shows a very small amount of absorption at a lower energy level, which changes the n and k values. These values have a significant influence on the calculated transmission spectra. We calculated the transmission for normal incidence using the following equation [33]:

$$T = \frac{Ax}{B - Cx + Dx^2} \tag{3}$$

The A, B, C, D, and x variables depend on the refractive index, extinction coefficient, thickness, and absorption coefficient of the polymer thin film at their respective wavelengths, as well as the substrate's refractive index. The equations used to calculate those values were given elsewhere [33]. The n and k of the thin film were obtained using the GEN-OSC model by fitting the SE data and refractive index of

the glass substrate obtained using the Cauchy model. Besides determining the optical properties from the SE model, we applied analytical methods to identify the same properties. In Fig. 3(a), we observed that the absorption edges are independent of thickness but do not follow the same spectral line for all thicknesses because the absorption properties depend on sample-making conditions such as the materials concentration, the curing process and the spin-coating recipe.

4. Conclusions

In this research, we determined the refractive index, extinction coefficient, and thickness of the PPDT2FBT polymer thin film on a glass substrate using spectroscopic ellipsometry. We used Psemi-Tri oscillators to generate the peak energies and matched those energy peaks with the absorption energy peaks, thus confirming the reliability of the determined optical properties. We also demonstrated that the optical properties are not completely independent of the film's thickness or the film-making process. Finally, we determined the refractive index range to be 2.00 to 2.15 and the extinction coefficient range to be 1.14 to 1.39.

CRediT authorship contribution statement

Chandan Howlader: Conceptualization, Methodology, Software, Writing - original draft, Experimenting. Mehedhi Hasan: Conceptualization, Validation, Writing - review & editing. Alex Zakhidov: Writing - review & editing. Maggie Yihong Chen: Supervision, Writing - review & editing.

Declaration of competing interest

The authors declare that they have no known competing financial interests or personal relationships that could have appeared to influence the work reported in this paper.

Acknowledgements

This research was funded by NORTHRUP GRUMMAN, grant number 2322623. We would also like to extend our gratitude here to our labmates for their support and suggestions. Alexander Zakhidov and Mehedhi Hasan acknowledge financial support from National Science Foundation, EPMD grant 1906492, Department of Navy HBCU/MI Program, and ONR grant N000141912576.

Appendix A. Supplementary data

Supplementary data to this article can be found online at https://doi.org/10.1016/j.optmat.2020.110445.

References

- S.J. Ko, et al., Photocurrent extraction Efficiency near Unity in a thick polymer bulk heterojunction, Adv. Funct. Mater. 26 (19) (2016) 3324–3330.
- [2] H. Kang, et al., Determining the role of polymer molecular weight for highperformance all-polymer solar cells: Its effect on polymer aggregation and phase separation, J. Am. Chem. Soc. 137 (6) (2015) 2359–2365.
- [3] J.Y. Kim, T.L. Nguyen, H. Choi, S.-J. Ko, M.A. Uddin, B. Walker, S. Yum, J.-E. Jeong, M.H. Yun, T.J. Shin, S. Hwang, "Semi-crystalline photovoltaic polymers with efficiency exceeding 9% in a ~300 nm thick conventional single-cell device, Energy Environ. Sci. 7 (9) (2014) 3040–3051.
- [4] C.W. Koh, et al., Enhanced Efficiency and long-term Stability of perovskite solar Cells by synergistic Effect of nonhygroscopic Doping in conjugated polymer-based hole-transporting layer, ACS Appl. Mater. Interfaces 9 (50) (2017) 43846–43854.
- [5] S. Yoon, C.W. Koh, H.Y. Woo, D.S. Chung, Systematic optical Design of constituting Layers to realize high-performance red-selective thin-film organic photodiodes, Adv. Opt. Mater. 6 (4) (2018) 1–6.
- [6] T.L. Nguyen, et al., Ethanol-processable, highly crystalline conjugated Polymers for eco-friendly Fabrication of organic Transistors and solar cells, Macromolecules 50 (11) (2017) 4415–4424.
- [7] J. Lee, et al., Highly crystalline low-bandgap polymer nanowires towards highperformance thick-film organic solar cells exceeding 10% power conversion efficiency, Energy Environ. Sci. 10 (1) (2017) 247–257.
- [8] T.H. Lee, et al., A universal processing additive for high-performance polymer solar cells, RSC Adv. 7 (2017) 7476–7482.
- [9] S.J. Ko, et al., High-efficiency photovoltaic cells with wide optical band gap polymers based on fluorinated phenylene-alkoxybenzothiadiazole, Energy Environ. Sci. 10 (6) (2017) 1443–1455.
- [10] M. Losurdo, et al., Spectroscopic ellipsometry for characterization of organic semiconductor polymeric thin films, Synth. Met. 138 (1–2) (2003) 49–53.
- [11] A. Lehmuskero, M. Kuittinen, P. Vahimaa, Refractive index and extinction coefficient dependence of thin Al and Ir films on deposition technique and thickness, Optic Express 15 (17) (2007) 10744.
- [12] X. Ziang, et al., Refractive index and extinction coefficient of CH_3NH_3Pbl_3 studied by spectroscopic ellipsometry, Opt. Mater. Express 5 (1) (2015) 29.
- [13] J.M. Ziebarth, M.D. McGehee, Measuring the refractive indices of conjugated polymer films with Bragg grating outcouplers, Appl. Phys. Lett. 83 (24) (2003) 5092–5094.

- [14] S.B. Khan, S. Irfan, Z. Zhuanghao, S.L. Lee, Influence of refractive index on antireflectance efficiency of thin films, Materials 12 (9) (2019) 8–10.
- [15] Hiroyuki Fujiwara, Spectroscopic Ellipsometry Principle and Application, John Wiley & Sons, LtdSP, 2007.
- [16] C.E. Petoukhoff, D.M. O'Carroll, Absorption-induced scattering and surface plasmon out-coupling from absorber-coated plasmonic metasurfaces, Nat. Commun. 6 (2015) 1–13.
- [17] C. Howlader, M. Hasan, A. Zakidov, M.Y. Chen, "Optical Dispersion Study of PPDT2FBT by Spectroscopic Ellipsometry," Proc. SPIE 11277, in: Organic Photonic Materials And Devices, vol. XXII, 2020, 1127712.
- [18] A. Yang, M. Bai, X. Bao, J. Wang, W. Zhang, Investigation of Optical and dielectric Constants of organic-inorganic CH3NH3PbI3 perovskite thin films, J. Nanomed. Nanotechnol. 7 (5) (2016) 5–9.
- [19] P. Löper, et al., Complex Refractive index Spectra of CH3NH3PbI3 Perovskite Thin Films determined by spectroscopic ellipsometry and spectrophotometry, J. Phys. Chem. Lett. 6 (1) (2015) 66–71.
- [20] S. Seifert, P. Runge, Revised refractive index and absorption of In1-xGaxAsyP1-y lattice-matched to InP in transparent and absorption IR-region, Opt. Mater. Express 6 (2) (2016) 629.
- [21] S.M. Eichfeld, C.M. Eichfeld, Y. Lin, L. Hossain, J.A. Robinson, Rapid, non-destructive evaluation of ultrathin WSe2 using spectroscopic ellipsometry, Apl. Mater. 2 (2014) 1–6, 092508.
- [22] M. Hasan, K. Lyon, L. Trombley, C. Smith, A. Zakhidov, Thickness measurement of multilayer film stack in perovskite solar cell using spectroscopic ellipsometry, AIP Adv. 9 (12) (2019).
- [23] A. Ng, et al., Accurate determination of the index of refraction of polymer blend films by spectroscopic ellipsometry, J. Phys. Chem. C 114 (35) (2010) 15094–15101.
- [24] B. Johs, J.S. Hale, Dielectric function representation by B-splines, Phys. Status Solidi Appl. Mater. Sci. 205 (4) (2008) 715–719.
- [25] B. Laboratories, M. Hill, F. Hottier, Investigation of effective-medium models of microscopic surface roughness by spectroscopic ellipsometry, Phys. Rev. 20 (8) (1979) 3292–3302.
- [26] I.J.A. Woollam Co, Guide To Using WVASE Spectroscopic Ellipsometry Data Acquisition And Analysis Software, 2011.
- [27] O.P.M. Gaudin, I.D.W. Samuel, S. Amriou, P.L. Burn, Thickness dependent absorption spectra in conjugated polymers: Morphology or interference? Appl. Phys. Lett. 96 (5) (2010) 3–5.
- [28] M. Mazumder, R. Ahmed, M. Hasan, S.J. Lee, M.S. Lee, Spectroscopic Ellipsometry of asphalt binder: a Study of optical constants, Int. J. Civ. Eng. 18 (3) (2020) 251–259
- [29] A.S.A. Aly, ALLAA. A, "Influence of film thickness on optical absorption and energy gap of thermally evaporated CdS0.1Se0.9 thin films, Chalcogenide Lett. 12 (10) (2015) 489–496.
- [30] A. Bedia, F.Z. Bedia, M. Aillerie, N. Maloufi, B. Benyoucef, Influence of the thickness on optical properties of sprayed ZnO hole-blocking layers dedicated to inverted organic solar cells, Energy Procedia 50 (2014) 603–609.
- [31] J.A. Woollam, Co, CompleteEase Software Manual, 2011, Version 4.63.
- [32] J. Jaglarz, A. Malek, J. Sanetra, Thermal dependence of optical parameters of thin polythiophene films blended with PCBM, Polymers 10 (4) (2018) 1–13.
- [33] D. Poelman, P.F. Smet, "Methods for the determination of the optical constants of thin films from single transmission measurements: a critical review, J. Phys. D Appl. Phys. 36 (2003) 1850–1857.